

Reflection of THz Radiation by a Superlattice

Avik W. Ghosh, Alex V. Kuznetsov, and John W. Wilkins

Department of Physics, The Ohio State University, 174 W. 18th Avenue, Columbus, Ohio 43210

(Received 7 July 1997)

Nonlinear THz reflection by a superlattice is calculated using an effective dielectric function. Oscillations of the reflection coefficient with the electric field amplitude signifies dynamic electron localization. The nonlinear connection between the incident and internal fields leads to a reflection coefficient exhibiting hysteresis as a function of the incident field. [S0031-9007(97)04415-3]

PACS numbers: 73.61.-r, 78.66.-w

The dynamics of a charged particle in a superlattice under the action of an external electric field has been the subject of intense research [1–6]. Under different conditions, an electron is predicted to reveal a variety of time-dependent phenomena such as Bloch oscillations [1], Zener tunneling [2], self-induced transparency [3], miniband collapse [4], negative differential conductivity, and absolute negative conductance in photon-assisted tunneling experiments [5], and other effects. In particular, the phenomenon of dynamic localization [6] is quite interesting. In the presence of a high frequency electric field $E(t) = E \cos(\omega t)$ along the growth direction of a superlattice of period d , an electron in a single miniband is predicted in general to drift off. However when the parameter $\Theta = eEd/\hbar\omega$ is a root of the zeroth order Bessel function, the electron is predicted to oscillate with a finite amplitude (in all of the following, we shall set $\hbar = 1$). Such a bounded motion at certain discrete parameter values can be understood in the following simple way: in each half-period of the incident ac field, the electron tries to execute Bloch oscillations. If it completes an integer number of Bloch oscillations before the sign of the field switches, the electron is localized, else it drifts off.

This sharp change in transport properties of the electron should be expected to show up in easily measurable optical properties. So far, the only observations of dynamic localization have been in photon-assisted tunneling experiments [5], where one observes the appearance of sidebands with intensity $J_n^2(\Theta)$, and in the parametric suppression of dc current in the presence of an ac field [7]. However, it is difficult to directly measure transport properties because one cannot simply attach electrical contacts to the superlattice and apply a voltage at THz frequencies. The only realistic way of applying THz frequency fields to a superlattice is to place the superlattice in the path of a propagating THz pulse. This argues for a more direct measurement of the optical properties of the superlattice at THz frequencies. With this in mind, we propose in this paper an optical experiment where one measures the THz reflection coefficient of the superlattice. We predict oscillations in the reflection coefficient as a function of the electric field amplitude arising out of dynamic electron localization. Previous theoretical studies of electronic re-

sponse to THz fields ignore where the electric field comes from and how it gets into the superlattice. The transformation between the field in the sample and the field outside is highly nonlinear, and leads, as we shall see, to a highly multistable behavior of the electronic response.

Dipole moment.—In a superlattice of period d , we consider motion only in the growth direction. For a single miniband of bandwidth Δ , the energy dispersion with respect to wave vector k is of the tight-binding form:

$$\epsilon_k = -\frac{\Delta}{2} \cos(kd). \quad (1)$$

The external electric field couples to the electron through the dipole matrix element which can be shown to be of the following form:

$$\hat{\mu}(kk') = ie \frac{\partial}{\partial k} \delta_{kk'}. \quad (2)$$

This form, identical to that for a bulk semiconductor, will never be directly evaluated. In any integral involving it, no confusion will arise with taking the continuous derivative of the Kronecker delta function. With these definitions, the effective Hamiltonian for noninteracting miniband electrons in a time-dependent electric field $E \cos(\omega t)$ is

$$\hat{H} = \sum_k \epsilon_k c_k^\dagger c_k - E \cos(\omega t) \sum_{kk'} \hat{\mu}(kk') c_k^\dagger c_{k'}. \quad (3)$$

Here $c_k^\dagger(c_k)$ are the conventional electron creation (destruction) operators.

Central to our approach is the electric-field-driven time evolution of the density matrix in terms of the center of mass momentum $K \equiv (k + k')/2$ and relative momentum $q \equiv k - k'$:

$$N_{Kq} \equiv \langle \hat{N}_{Kq} \rangle \equiv \langle c_{K+q/2}^\dagger c_{K-q/2} \rangle, \quad (4)$$

We assume that the density matrix tends to relax to an equilibrium value N_{Kq}^0 with a relaxation time τ . We do not consider the detailed process by which electrons populate the conduction miniband (doping, photoexcitation). We simply start with an electron population in the conduction miniband having an initial distribution that is uniform between quasimomenta $\pm k_F$, given by

$N_{K0}^0 = n\pi/k_F[\theta(K + k_F) - \theta(K - k_F)]$, where θ is the Heaviside step function and n is the density of electrons in the conduction miniband. Our equations of motion then give us

$$\frac{\partial N_{Kq}}{\partial t} = -i[\epsilon_{K+q/2} - \epsilon_{K-q/2}]N_{Kq} - eE(t)\frac{\partial N_{Kq}}{\partial K} - \frac{N_{Kq} - N_{Kq}^0}{\tau}. \quad (5)$$

We compute the time-dependent dipole moment $\mu(t) \equiv \text{Tr}(\hat{\mu}N)$ from Eq. (5) and that for the dipole moment derived from it: $\partial\mu/\partial t + \mu/\tau = e\sum_K v_K N_{K0}$, where $v_K \equiv \partial\epsilon_K/\partial K$ is the velocity of the electrons. Note that the equation for the dipole moment requires only the value of N_{Kq} at $q = 0$. We then get an expression for the dipole moment in terms of the dimensionless electric field amplitude $\Theta \equiv eEd/\omega$ [8]:

$$\mu(t) = -\frac{ed\Delta}{\omega} J_0(\Theta) \sum_{m=0}^{\infty} \frac{J_{2m+1}(\Theta)}{2m+1} \cos[(2m+1)\omega t]. \quad (6)$$

At those values of Θ where $J_0(\Theta) = 0$, the time-dependent dipole moment vanishes. For a different initial condition, such as a steady-state current, at the zeros of $J_0(\Theta) = 0$ the dipole moment has bounded oscillations. These are both examples of dynamic localization of electrons.

Reflection coefficient.—The inset in Fig. 1 shows a possible experimental setup: Incident THz radiation is polarized along the growth direction of the superlattice, and the reflected beam is examined for signatures of dynamic localization of electrons. Consider the idealized problem of a monochromatic incident wave propagating monochromatically into a superlattice infinitely extended along the growth direction. We neglect the fact that in an actual geometry, the spot size is usually a hundred times larger than the superlattice length along the growth direction, which means that a large part of the monitored reflection arises out of the substrate rather than the superlattice itself [9].

By omitting the higher harmonics generated in Eq. (6) [10], we can define an effective dielectric function as obtained from the coefficient of $\cos(\omega t)$:

$$\epsilon_{\text{eff}}(\Theta) = \epsilon_0 \left[1 - 2 \frac{\omega_P^2}{\omega^2} \frac{J_0(\Theta)J_1(\Theta)}{\Theta} \right]. \quad (7)$$

Here ϵ_0 is the static (dc) dielectric constant of the superlattice (~ 12.4 for GaAs), and $\omega_P \equiv \sqrt{4\pi ne^2/m^* \epsilon_0}$ is the plasma frequency of the electrons with an effective mass $m^* \equiv \Delta/2d^2$. For low values of Θ , this reduces to the dielectric constant for plasmons, viz. $\epsilon_{\text{eff}}|\Theta| = \epsilon_0[1 - \omega_P^2/\omega^2]$.

Figure 1 shows the reflection coefficient resulting from a straightforward application of this effective dielectric function [11]. With respect to the background (dashed line in Fig. 1), the reflection coefficient is zero at the same values of the electric field previously identified

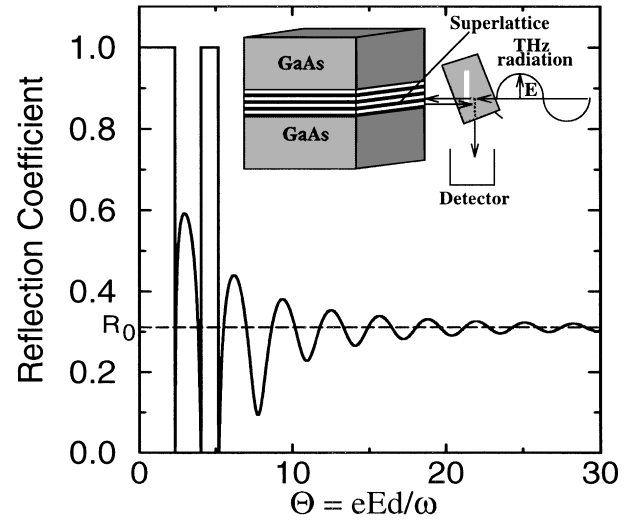


FIG. 1. Predicted reflection coefficient of a superlattice in a THz field, plotted vs the dimensionless electric field amplitude at the site of the electron eEd/ω , for $\omega_P/\omega = 8$. At high fields, the electronic contribution to the reflection coefficient vanishes, while at low fields, the field is screened by the plasmons since the incident frequency ω is less than the plasma frequency ω_P . There is a window of low reflection coefficient in the low-field regime. When $J_0(eEd/\omega) = 0$, the reflection coefficient reaches the background value $R_0 = |(\sqrt{\epsilon_0} - 1)/(\sqrt{\epsilon_0} + 1)|^2$ because the electrons dynamically localize, and do not radiate. Inset: Schematics of the proposed THz optical experiment. The superlattice is sandwiched between substrates of GaAs and the incident THz radiation is polarized along the growth direction. The reflected radiation is collected using a partially transmitting mirror and analyzed for signatures of dynamic localization.

with dynamic localization. Three special features of this computed reflection coefficient are worth noting: (1) The “self-induced transparency” effect [3] actually corresponds to a vanishing of the *electronic* contribution to the THz reflection coefficient at the Bessel roots—the background contribution still remains. At nearby values of Θ , the background reflection coefficient destructively interferes with the electronic part and the total reflection coefficient actually drops below the dc value; (2) the oscillatory behavior of the reflection coefficient and (3) the sharp drop in its value for low fields. For *low* electric fields the system is expected to behave like a metal, the electrons executing plasma oscillations which screens the field, since $\omega_P > \omega$. The predicted reflection coefficient is unity over a range of low Θ 's, but there is a sharp drop in reflection coefficient in the middle of this range near the first Bessel root, where the electrons dynamically localize. At *large* values of the field amplitude, the electric field overcomes plasmon screening, and the reflection coefficient is controlled essentially by the dc dielectric constant ϵ_0 , since the Bessel functions in Eq. (7) vanish for large values of their arguments. Thus the THz reflection coefficient reaches the dc value $R_0 = |(\sqrt{\epsilon_0} - 1)/(\sqrt{\epsilon_0} + 1)|^2$.

Actual field in the sample.—Figure 1, however, does not give us the complete picture. Relevant experimental prediction requires reflection coefficient as a function not of the electric field E at the site of the electron, but rather the external field E_I incident on it. Before we make experimental predictions, we need to perform a transformation of variables from $\Theta_S \equiv eE_S d/\omega$ to $\Theta_I \equiv eE_I d/\omega$, E_S being the field amplitude in the sample. This transformation causes the reflection coefficient to exhibit hysteretic behavior.

The variables E_S and E_I are connected via boundary conditions at $x = 0$, viz.,

$$\Theta_I - \Theta_R|_{x=0} = \Theta_S|_{x=0}, \quad (8)$$

$$\frac{\partial}{\partial x}(\Theta_I - \Theta_R)|_{x=0} = \frac{\partial \Theta_S}{\partial x}|_{x=0}, \quad (9)$$

where $\Theta_R \equiv eE_R d/\omega$, with E_R being the reflected field amplitude at the boundary. Here x is the direction of propagation of the incident wave. We now need the x dependence of the boundary value Θ_S , to substitute in Eq. (8) (and to know the electronic contributions to the reflection from different positions x). The position dependence of the field E_S is obtained by solving the wave equation in the sample. Ignoring higher harmonics, the wave equation can be written as

$$\frac{\partial^2 \Theta_S(x)}{\partial x^2} = -\epsilon_{\text{eff}}[|\Theta_S(x)|] \frac{\omega^2}{c^2} \Theta_S(x). \quad (10)$$

In Eq. (10), we emphasize that ϵ_{eff} depends only on the modulus of the amplitude of the field. This imposes a self-consistency condition on (10), because the dielectric function in the equation depends on the solution to the equation. We identify two main types of x dependences: (A) *propagating*: $|\Theta_S(x)| = \text{const}$, which holds for $\epsilon_{\text{eff}}[|\Theta_S(x)|] > 0$; and (B) *decaying*: $|\Theta_S(x)| = \Theta_S(x)$, with $\partial \Theta_S(x)/\partial x|_{x=0} < 0$, for $\int_0^{\Theta_S(x)} \epsilon_{\text{eff}}(y) y dy < 0$.

Figure 2 shows the two branches (A) and (B), in a conversion plot between the variables Θ_S and Θ_I . For a given value of E_I there are several possible values of E_S and thus of the reflection coefficient. The oscillations in the propagating branch of the figure arise directly out of the Bessel oscillations in $\epsilon_{\text{eff}}(\Theta_S)$ [Eq. (7)]. The experimentally controlled parameter is Θ_I . We get a strongly multistable electronic response merely because we monitor reflection coefficient in terms of the parameter Θ_I instead of Θ_S , and the transformation between the two is controlled by the highly nonlinear effective dielectric function ϵ_{eff} .

Figure 3 shows the effect of the nonlinear transformation of Fig. 2 on the reflection coefficient in Fig. 1, with Θ replaced by Θ_S . The reflection coefficient exhibits pronounced structure, with switchings between branches. The sawtooth form of the resultant reflection coefficient is a clear signature of dynamic localization. Owing to the nonlinear transformation associated with the penetration of the field into the superlattice, dynamic localization does

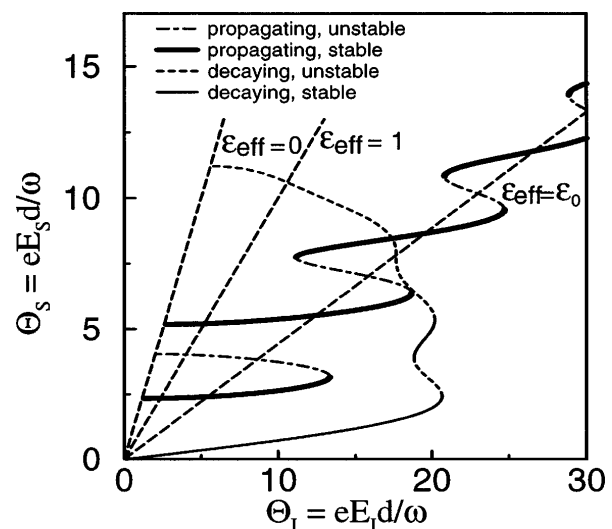


FIG. 2. Change of variables from field at the boundary inside sample (E_S) to field outside (E_I). There are two branches corresponding to propagating and decaying fields in the sample. When the propagating branch crosses the straight line corresponding to $\epsilon_{\text{eff}} = 1$, the reflection coefficient drops to zero. The transformation is nonunique, owing to a highly nonlinear electronic response. The curves are bounded on one side by the line corresponding to $\epsilon_{\text{eff}} = 0$. The propagating branch asymptotically reaches the line corresponding to $\epsilon_{\text{eff}} = \epsilon_0$.

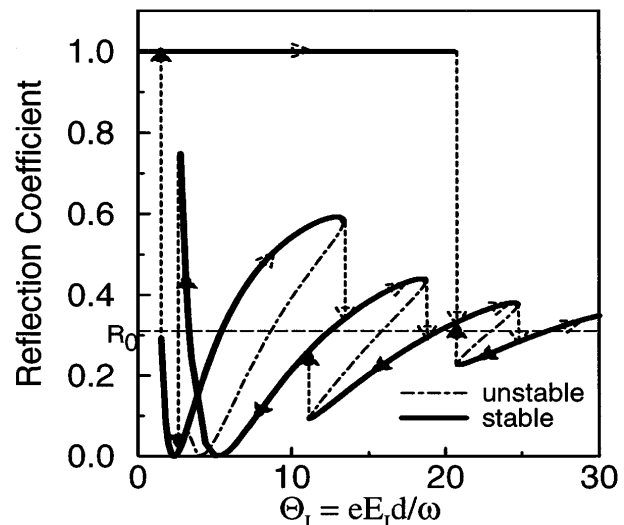


FIG. 3. THz reflection coefficient of a superlattice plotted vs the dimensionless incident electric field at the boundary $\Theta_I = eE_I d/\omega$. The stable (solid line) and unstable (dot-dashed line) branches have been indicated on the graph. There are prominent oscillations which are skewed versions of those in Fig. 1. As Θ_I is increased from zero, the reflection coefficient starts off from unity, till it drops sharply to the background value and follows the sawtooth shape indicated by the hollow arrows. On decreasing Θ_I from high values, the reflection coefficient follows a different sawtooth indicated by the filled arrows. This behavior is a direct consequence of dynamic localization and strong multistability arising out of highly nonlinear electronic response.

not occur at the Bessel roots of the incident field, as one may naively expect. The switchings between the branches occur at different values of E_I depending on whether the incident field amplitude is increasing or decreasing, yielding hysteresis loops. Also note a sharp switch in reflection coefficient from unity to R_0 , which is a drop that should be easily measurable.

In the above calculations, we have completely ignored the effect of any electron-electron interaction (by setting $\omega\tau \rightarrow \infty$) and considered a strict cosine dispersion of our miniband. Corrections to the dispersion rule are not expected to change the qualitative features of the reflection coefficient [12]. Within a relaxation-time approximation, collisions change our results only to $O(1/\omega^2\tau^2)$ and the dynamic localization points are shifted. Finally, reintroducing the higher harmonics merely produces high frequency oscillations atop those in Fig. 3.

We have addressed the problem of a plane THz wave reflecting off an infinitely long superlattice. We see that the realistic means by which the field penetrates the superlattice is important, and in fact leads to a bistable/multistable response. We demonstrate that dynamic localization of electrons leads to dramatic features in the optical properties of the superlattice, at input fields that are related to dynamic localization conditions by a nonlinear transformation.

This work was supported by the Office of Naval Research.

[1] F. Bloch, Z. Phys. **52**, 555 (1929).

[2] J. Rotvig, A.P. Jauho, and H. Smith, Phys. Rev. Lett. **74**, 1831 (1995).

[3] A. A. Ignatov and Yu. A. Romanov, Sov. Phys.-Solid State

17, 2216 (1976).

[4] M. Holthaus, Phys. Rev. Lett. **69**, 351 (1992).

[5] B. J. Keay, S. Zeuner, S. J. Allen, Jr., K. D. Maranowski, A. C. Gossard, U. Bhattacharya, and M. J. W. Rodwell, Phys. Rev. Lett. **75**, 4102 (1995).

[6] D. H. Dunlap and V. M. Kenkre, Phys. Rev. B **34**, 3625 (1986).

[7] S. Winnerl, E. Schomburg, J. Grenzer, H. J. Regl, A. A. Ignatov, K. F. Renk, D. P. Pavel'ev, Yu. Koschurinov, B. Melzer, V. Ustinov, S. Ivanov, S. Schaposchnikov, and P. S. Kop'ev, Superlattices Microstruct. **21**, 91 (1997).

[8] In computing $\mu(t)$, we first drop the transients ($t \gg \tau$), and then ignore collisions, assuming $(\omega\tau)^2 \gg 1$. Typical values for a continuous wave free electron laser are $\omega \sim 1-10$ THz, $\tau \sim 1$ ps, and pulse length ~ 1 μ s, which satisfies the above inequalities pretty well. Note that if we drop the collision term *before* dropping the transients, we do not get the prefactor $J_0(\Theta)$ that is so crucial to dynamic localization.

[9] One way of making the substrate reflection unimportant is to monitor the far-field reflection coefficient at higher harmonics [12], which arise only out of the superlattice. At long distances, the detector does not interfere with the incident radiation.

[10] An approximate implementation of a method suggested by L. J. F. Broer, Phys. Lett. **4**, 65 (1963) allows an alternate calculation of the reflection coefficient, where we retain higher harmonics and solve analytically for the reflection coefficient for large and small values of Θ and establish an interpolation scheme between the two limits. The resulting reflection coefficient has the same structure as Fig. 1 with additional high frequency wiggles resulting from the higher harmonics [12].

[11] J. D. Jackson, *Classical Electrodynamics* (John Wiley and Sons, Inc., New York, 1975), Eq. (7.42), p. 282.

[12] A. W. Ghosh, A. V. Kuznetsov, and J. W. Wilkins (to be published).